PAPER • OPEN ACCESS

Impact of rooftop stack configuration on 2D street canyon air quality

View the article online for updates and enhancements.
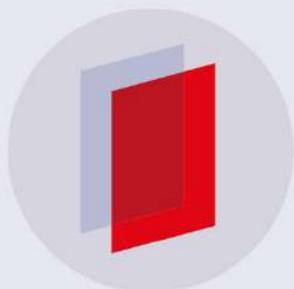
Impact of rooftop stack configuration on 2D street canyon air quality

M G Badas[1]**, M Garau**[1]**, A Seoni**[1]**, S Ferrari**[1] **and G Querzoli**[1*]

[1]DICAAR - Dipartimento di Ingegneria Civile, Ambientale e Architettura.
Università degli Studi di Cagliari, via Marengo 2, 09123 Cagliari, Italy

*querzoli@unica.it

Abstract. We experimentally investigated the impact of rooftop stack position on the pollutant entrapment within 2D street canyon configurations. Analyses were performed in a water channel loop system by using the image analysis techniques: FTV (Feature Tracking Velocimetry) and LIF (Light Induced Fluorescein) respectively for measuring velocity and concentration. The set-up consists in an array of 20 identical buildings with aspect ratio equal to one ($AR_B = B/H$, where H is the height of the eaves and B is the building width), mimicking an idealized 2D urban canopy. They were equally spaced with a unitary canyon aspect ratio (defined as $AR_C = W/H$; where W is the distance between buildings facades), and varied in shape by using flat and gable roofs with pitch $\alpha = 45°$, with different chimney positions and heights, for a total number of 9 investigated configurations. Results demonstrate that the presence of gable roof significantly varies the flow in the shear layer, which, in combination with different chimney position and height, lead to not trivial effects on pollutants dispersion.

1. Introduction

The urban canopy is characterized by a complex geometry that interacts with the fragile equilibrium governing atmosphere, soil and subsoil system. Cities are usually characterized by elevated sources of heat and pollutants, and high levels of PM10 and PM2.5, NO2, SO2, carcinogenic hydrocarbons, etc., which are potentially dangerous for human health. Ventilation has a crucial role against their retention in the urban canopy layer: it promotes the removal of pollutants and heat by means of both the mean flow and the turbulence.

Several studies have been undertaken, both experimentally and numerically, to investigate the pollutant dispersion in the urban boundary layer from the street-scale (~100–200 m) to the district-scale (~1–2 km), (Britter and Hanna 2003) and with different specific objectives. Most of these analyses were based on simplified building geometries and configurations (e.g. Di Bernardino et al. 2017) with the aim to understand the single element influence. However, real urban patterns are more complex and other parameters, such as the variability of building height and shape (e.g. Nosek et al. 2017; Garau et al. 2018b), intersections (Carpentieri et al. 2012; Nosek et al. 2016), presence of trees, building density, etc., deeply influence the flow and pollutant dispersion. The sensitivity of urban area models to geometrical simplifications is a fundamental issue for air flow modelling (Ricci et al. 2017),

and the choice of a proper modelling configuration might have even more important implications for dispersion simulations.

Most of published papers in urban context deal with contaminants dispersed at the street level, since traffic is generally the most important pollution source. Nonetheless, dispersion from stacks, which is typically associated with industrial and open country context, may be important also in cities. For instance, Ghermandi et al. (2015) presented a micro-scale simulation of stack dispersion from a tri-generation power plant, designed to supply the energy demand of the Modena General Hospital (Italy).

In this perspective, it is important to assess the reliability of adopted simulation models in urban context. To pursue this issue, it is fundamental to perform laboratory experiments, in controlled and repeatable conditions, for simplified urban set-ups.

Most current dispersion models assess the pollutant concentration further away from the release, while they have severe limitations for near field prediction. Traditionally, dispersion from industrial stacks is modelled by means of Gaussian models while ASHRAE geometric stack design method and models are often used in order to assess a proper stack height.

Even in the simpler case of a single building, the situation is far from being simple. Schulman et al. (2000) showed the effect of stack proximity to a structure on plume dispersion. Saïd et al. (2005) highlighted, in case of a stack placed on the top of an isolated single building, the complex interaction between the plume wake and the recirculating region behind the building, and the downwash effect due to the cross-flow on the top of the chimney, which depends on approaching wind conditions.

Saathoff et al. (2009) investigated in a wind tunnel model the roof key role in near field dispersion, in case of a rooftop stack located downwind a single building. They varied building heights, rooftop structure and wind directions and compared results with ASHRAE models, pointing out their weakness in some of the adopted configurations. Hajra et al. (2010) studied dispersion of building exhaust pollutants in case of a high-rise building and a low-rise building using both wind tunnel and numerical modelling (ADMS, ASHRAE), and highlighting severe limitations of the latter for some of the adopted configurations.

Few studies were performed considering more than a single building. Bagieński (2006) performed a laboratory simulation of a single street canyon (considering two flat building, and the three cases of symmetric, step-up and step-down canyon) showing how the canyon pollution is affected by building configuration and source position. Dispersion from rooftop stacks in presence of an urban canopy, to the best of authors knowledge, has not been addressed in literature. Actually, urban building and roof geometrical configuration role, in attenuating or worsening canyon pollution, might be of opposite sign with respect to cases where the contaminant is released at the street level.

Actually, the plume behavior is affected by many factors, apart from the surrounding area, the plume buoyancy and the atmospheric conditions. For instance, in their pioneering work, Willis and Deardorff (1983) showed how a stack emission evolves in case of a Convective Boundary Layer, a situation where more complex spatial structures also in case of flat terrain (Badas and Querzoli 2011).

The present work is aimed at investigating dispersion from a stack in urban canyons, in the simplest case of a perpendicular incident wind and negligible buoyancy effects. A series of experimental simulations considering variable chimney configuration (height and position above roofs) is here presented for flat and gable roof buildings, having a square section and a unitary canyon aspect ratio.

Results show the complex interaction between the plume and the underlying urban canyon, which may lead to unexpected results in terms of canyon pollution.

2. Experimental Set-Up

2.1. Water channel facility
Flow in urban canyon configurations is investigated by means of a water channel, at the Hydraulics Laboratory of the University of Cagliari. The facility, sketched in Fig.1, consists of a $8.0\,m$ long

channel with a rectangular section $0.40\,m$ wide and $0.50\,m$ deep. A constant-head reservoir was positioned at the inlet section and the mean velocity was regulated by a sharp-crested weir at the end of the channel. A turbulent boundary layer of $\delta = 0.42\,m$ depth with the free stream velocity equal to $U_{ref} = 0.36\,m/s$ was obtained via a $0.10\,m$ thick honeycomb, placed at the inlet section, and a series of $3.0\,m$ panels covered with pebbles, having a mean size of $5\,mm$. The approaching flow characteristics were defined by a series of preliminary measurements and discussed in details in Garau et al. (2018a). In order to investigate the idealized 2D canopy, a series of 20 identical buildings was located after the pebbles panels, hence the measuring section was positioned $6.15\,m$ downstream from the honeycomb. Buildings were modelled as prismatic obstacles (with a squared section of $20\,x\,20\,mm$ and the same section with an overlying $45°$ gabled roof), while the span-wise width was equal to the channel one. The adopted configuration allows achieving a blockage ratio smaller than 5% (as prescribed in Barlow et al. 1999). The measuring section corresponded to the 17th canyon, ensuring that the roughness layer reached the equilibrium (Brown et al. 2000; Llaguno-Munitxa et al. 2017) and that results were representative of an infinite series of identical canyons. Buildings, equally spaced by street canyons of aspect ratio equal to 1 (where the aspect ratio is defined as the ratio of the canyon width W to the building height H, $AR_C = W/H$) and schematically reported in Fig.2b, were performed with flat roofs and gabled roofs with $45°$ pitch. Furthermore, chimneys with three different heights (h = 5, 10, 15 mm, corresponding to the non-dimensional size h/H = 0.25, 0.5, 0.75) and different positions above the roofs (leeward and windward sides for gabled roofs and the central point in case of flat roof, as sketched in Fig. 2 a), were simulated. The three different chimney heights employed, correspond to the lower, equal and higher height with respect to the top of the building with roof. The total number of analysed configurations was 9 as reported in Table 1.
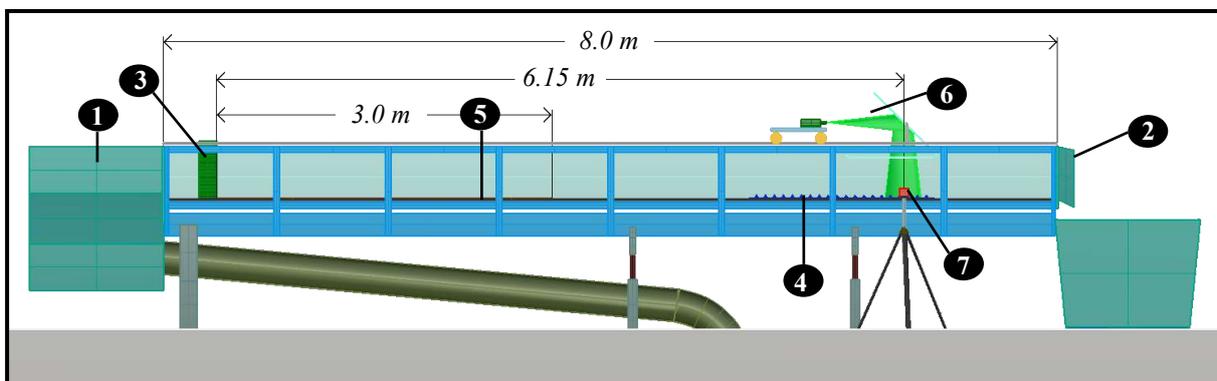

Figure 1: sketch of the water channel facility. (1) Constant head reservoir; (2) sharp-edged weir; (3) honeycomb; (4) array of 20 buildings; (5) 3 m pebbles panels; (6) laser and mirror; (7) high-speed camera.
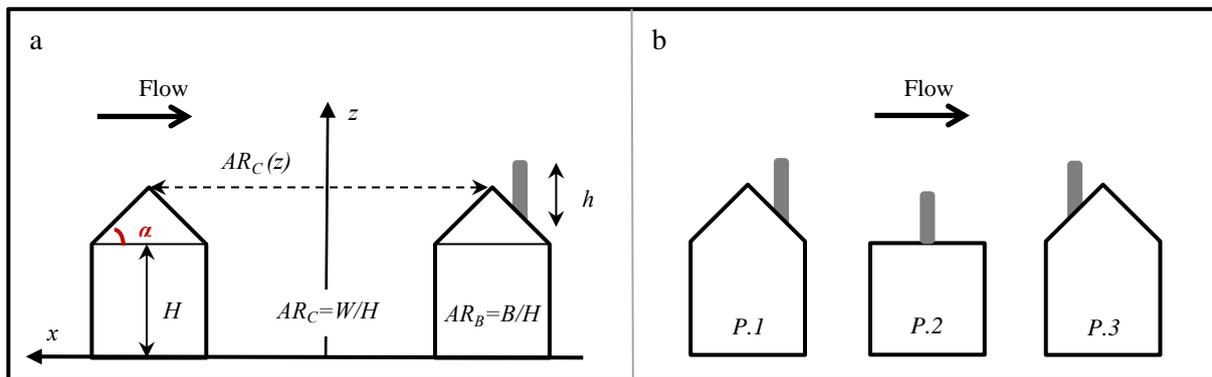
Figure 2: (a) schematic representation of buildings: α=pitch roof angle, h=chimney height, H=building height, B=building width, W=canyon width, AR$_C$=canyon aspect ratio, AR$_B$=building aspect ratio. (b) three chimney positions respect to wind direction: P.1=leeward side, P.2=central point, P.3=windward side.

The stream Reynolds number was found equal to $Re = UH/\nu = 151,000$, higher than the minimum requested by Snyder (1972), thus sufficient to guarantee the independence of the large turbulence structures of the flow on the Reynolds number.

Velocity and concentration measurements were performed using non-intrusive image analysis techniques, as described in next paragraphs.

Table 1: analysed configurations with different position and height for chimneys on the roof with variable pitch angles.

Chimney position on the roof	Chimney height: h/H		
	0.25	**0.5**	**0.75**
P.1 = leeward	45°	45°	45°
P.2 = centre	0°	0°	0°
P.3 = windward	45°	45°	45°

2.2. Velocity and turbulent field measurements

Velocity and turbulent field measurement were performed by means of the FTV (Feature Tracking Velocimetry), developed at the University of Cagliari (Besalduch et al. 2013, 2014). This is a non-intrusive technique, less problematic with respect to the common PIV (Particle Image Velocimetry) methods to the occurrence of high velocity gradients and to the appearance and disappearance of particles. This technique was already successfully employed for previous similar studies (e.g. Ferrari et al. 2016, 2017, where more details are found).

The fluid was seeded with pine pollen non-buoyant particles ($20 \, \mu m$ mean diameter), uniformly dispersed into the water before the experiments.

The measuring section corresponding to the mid section of the channel above the 17th street canyon, was lighted by means of a diode laser ($532 \, nm$ in wavelength and $2W$ in power) coupled with an optical system consisting of a lens and a mirror. A high-speed camera, $2240x1760$ pixels in resolution, was adopted to record at $310 \, Hz$, the investigation plane. For each of the analysed configurations, 40 measurements sessions were performed and a total number of 48,000 frames were employed for statistical analysis.

2.3. Concentration measurements

Concentration measurements were performed by means of fluorescence (LIF) technique: at low concentrations, fluorescein adsorbs and reemits light proportionally to dye concentration. In order to

minimize light non-homogeneities of the framed area, which could bias the obtained concentration fields, a representative number of frames (1500) was recorded prior to the experiment. The resulting background pattern was subtracted from each frame. Mean concentration fields were thus calculated by means of a total number of 7000 frames for each case with a high-definition camera ($1200x900$ pixels in resolution), a frequency of $25\,Hz$ and a time exposure of $1/250\,s$. The measuring section was lighted with a diode laser $473\,nm$ in wavelength and $1.5W$ in power. The fluorescein solution in water was stored in a reservoir with constant level and connected with a thin tube to the chimney having $1.7\,mm$ internal diameter width so that the flow rate was calculated as $0.03\,ml/s$. This rate well represents the behaviour of a vertical plume of pollutant with a negligible velocity with respect to the main flow. Concentration fields are analysed after being non-dimensional by dividing by the concentration at the source.

3. Results and Discussion

Mean and turbulent velocity fields are first shown and analysed to describe how the presence of a gable roof deeply affects the flow field. Afterwards, concentration fields are presented and discussed for the 9 sets-up simulated, corresponding to different chimney configurations, to get insight on the pollutant entrapment mechanism inside the canyon.

3.1. Flow fields

The mean stream-wise velocity field generated by flat and 45° gabled roof buildings, are compared in Fig.3. The adopted set-up and measurement technique was validated on both numerical and experimental literature works as reported in a previous work (Garau et al. 2018a). The superimposed streamlines highlight the well-known flow pattern for the skimming flow regime (Oke 1988). Indeed, a stable single vortex is established inside the canyon for both the configurations. However, the central point of the main vortex, positioned near $x/H = 0.0$ in accordance with literature works (e.g. Di Bernardino et al. 2015b), moves up along z direction for gabled roof and, in case of 45° slope, it appears close to the level of the eaves. As a consequence, stream-wise velocities decrease in the overlaying flow near the buildings top as well as inside the canyon, where a counter rotating vortex grows up in the windward facade of the building.
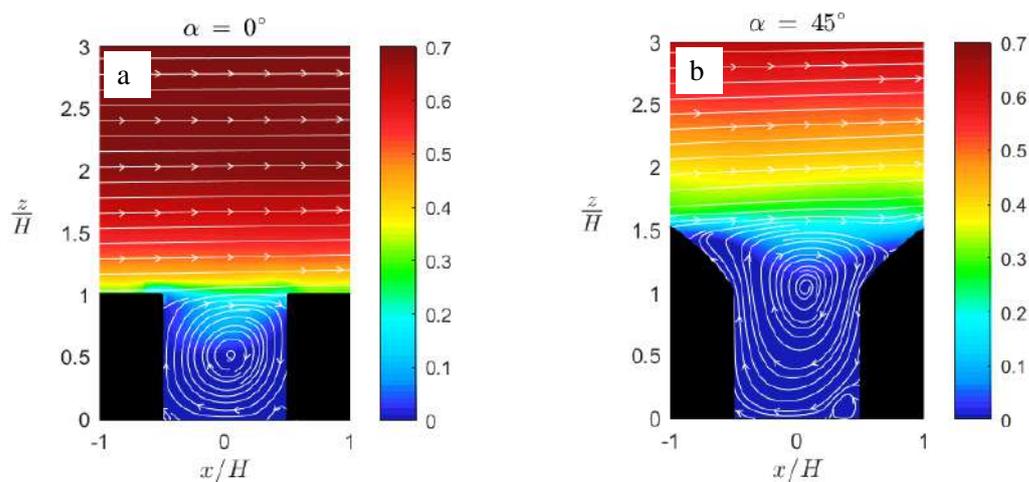

Figure 3: non-dimensional stream-wise velocity field overlapped by the streamlines of velocity field, for configurations with flat roofs (a) and gabled roofs (b). Colour scale is common for all the panels. Values are made non-dimensional by the free-stream velocity U_{ref} at z/H = 7.

Looking at the vertical velocity fields (Fig.4), the highest velocity values are in the lateral parts of the main vortex, near the building facades. In case of gabled roofs, these two well-defined regions are wider and shifted up around the eave corners. Thus, at pedestrian levels, vertical velocities are higher for flat roof configuration. Together with the turbulent quantities, the vertical velocity component is important because of the straight connection with ventilation mechanism, characterized by ventilation indexes such as the air-exchange rate ACH (Ho et al. 2015; Badas et al. 2017) or the mean and the total outflow ventilation rate (Garau et al. 2017).
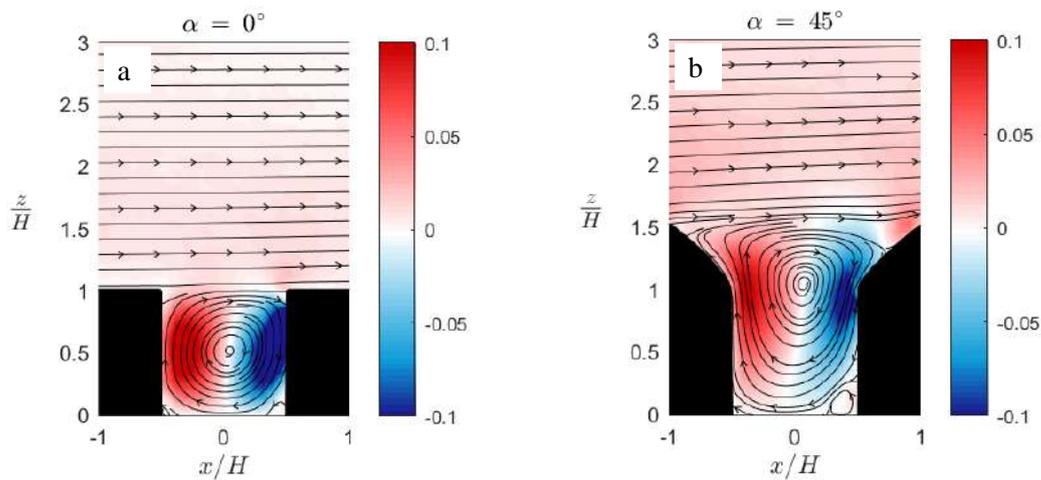

Figure 4: non-dimensional vertical velocity field overlapped by the streamlines of velocity field, for configurations with flat roofs (a) and gable roof. Colour scale is common for all the panels. Values are made non-dimensional by the free-stream velocity U_{ref} at z/H = 7.

An in-depth description of the modification of the turbulent fields going from flat roof to gable roof configuration and the implication for canyon ventilation are reported in Garau et al. (2018a). Here, as an example, turbulent kinetic energy fields are plotted in Fig.5. It is apparent how the roof presence affects the shear layer evolution, causing higher turbulence not only in the region above roofs but also in the intermediate region within the roof pitches and the eaves. Moreover, near the windward building a high turbulence tongue deeply extends into the canyon, enhancing the mixing between in and out canyon regions.
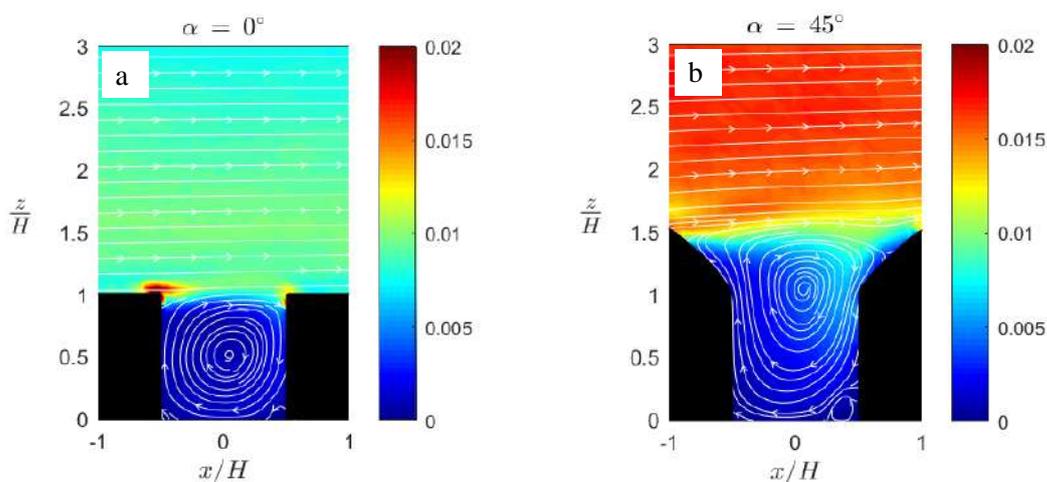

Figure 5: non-dimensional turbulent kinematic energy fields overlapped by the streamlines of velocity field, for configurations with flat roofs (a) and gable roof 45° sloped (b). Colour scale is common for all the panels. Values are made non-dimensional by the free-stream velocity U_{ref} at z/H = 7.
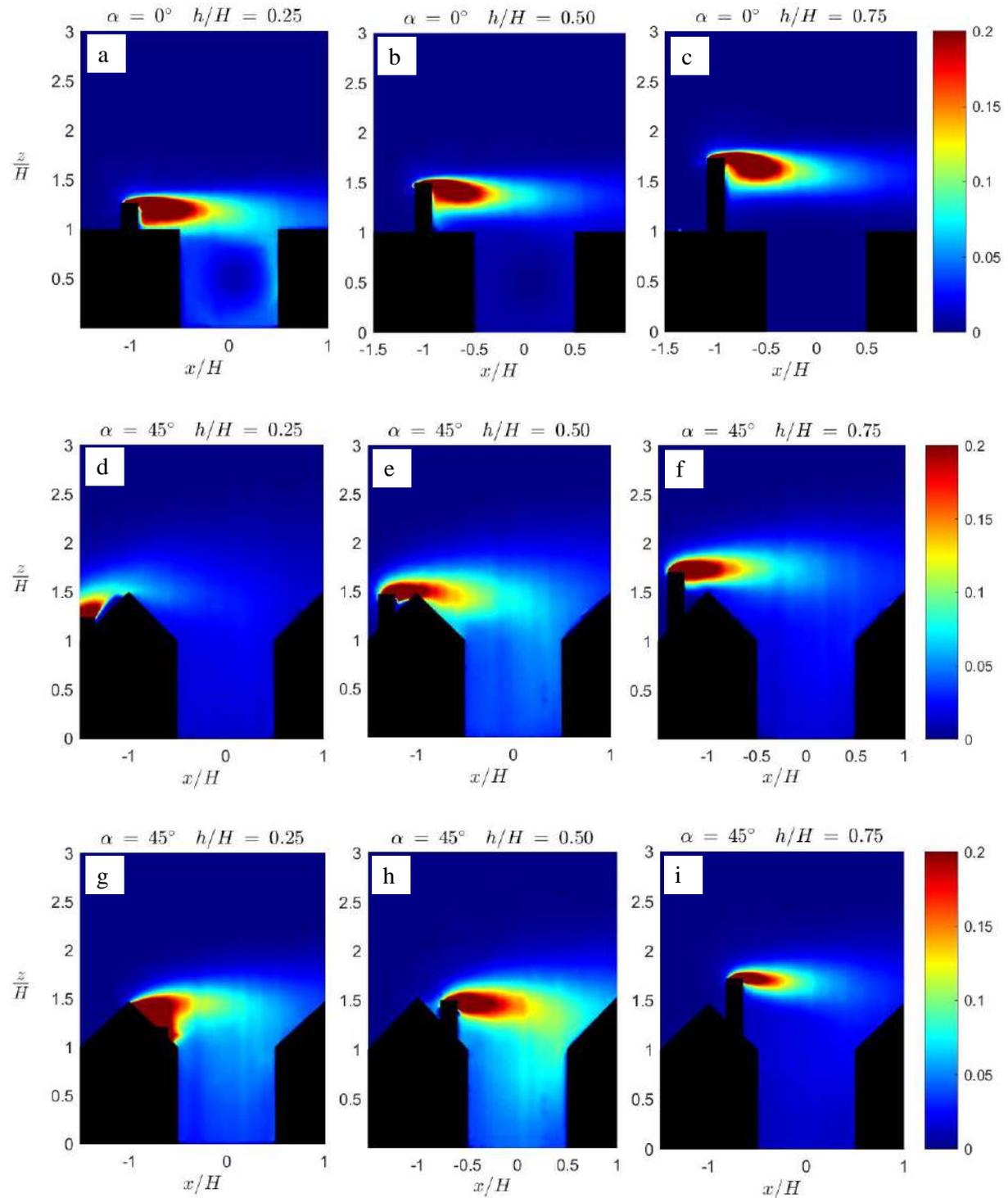
3.2. Concentration fields

Figure 6: mean concentration transport field made non-dimensional with the maximum concentration registered at the source point (white cross and green circle), for flat roof cases (a-c) and 45° gable roof cases (d-i) with three different chimney heights (h/H=0.25 for a, d, g,0.5 for b, e, h,0.75 for c, f, i) and three different position above the roof (central point for a-c, windward for d-f and leeward position for g-i).

Maps of concentration fields, made non-dimensional with respect to the maximum concentration at the source point (i.e. the chimney top), are shown in Figure 6 for all the 9 cases. Moreover, mean and standard deviation of concentration inside the canyon, defined as the region between the buildings, going from to the street to the height of the eaves, are displayed in Table 2.

Analysing results, a general trend with respect to stack height, common for flat and gable roof buildings does not emerge from Table 2 mean values. This suggests that the influence of chimney and the interaction generated with the roof shape, chimney height and position, have not trivial outcomes. Thus, we discuss results distinguishing the two roof shape configurations.

Table 2: Mean concentration and standard deviation values computed inside the canyon for the 9 analysed configuration.

Roof Angle	Chimney position	Statistics into the canyon	Chimney height: h/H		
			0.25	**0.5**	**0.75**
0°	P.2 = centre	mean	0.0336	0.0065	0.0004
45°	P.3 = windward	mean	0.0175	0.0411	0.0184
45°	P.1 = leeward	mean	0.0408	0.0550	0.0155

In the case of flat roofs, higher chimneys (Fig. 6 b-c) cause less interaction with the canyon interface, leading to very low entrainment, while in case of small chimney height (Fig. 6a) the plume highly interacts with the canyon below, and a tongue of polluted flow entering the canyon is clearly visible in the windward building corner. The plume axis, defined as the locus of maximal concentrations, is deflected toward the canyon with respect to the mean flow, particularly for the smaller chimney height case. Moreover, the canyon presence and the boundary layer structure lead to an asymmetric plume growth, which results in a larger widening with respect to its axis toward negative z direction.

In the case of gable roof, the best conditions are obtained, quite obviously, when the highest chimney is considered, irrespective of its position (Fig.6 f, i). These configurations correspond to less interaction between the plume and the canopy. However, due to the longer distance from the source as well as to the interaction with the upwind building roof, when the chimney is placed on the windward pitch (Fig. 6 f), the canyon interaction is more intense compared to the latter case (Fig.6 i), although mean concentration inside the canyon are quite comparable (see Table 2). For the other two chimney heights the source is released at lower levels with respect to the roof top, hence a stronger interaction is foreseen. For these configurations (Fig.6 d, e, g, h) the plume encounters the windward building roof and it is partially entrapped. Here, the chimney position plays a more important role: the canyon pollution worsens when the source is released in the leeward position (Fig.6 h) compared to the windward position (Fig.6 e). Actually, this is quite obvious since, considering the pitch height, the condition portrayed in Fig. 6e corresponds to the pollution released inside the canyon where we are measuring concentrations. Whilst all the maps display quite regular patterns, where the plume widens while being driven by the main flow direction, Fig.6 g shows an apparently awkward feature, since it displays a high concentration region upwind the chimney. This is due to the presence of the vortex, which extends close to the leeward roof pitch (Fig. 3b-5b), and whose streamlines are directed in the opposite way respect to the main flow in chimney region, so differently to the expected behaviour, lower mean concentration field in canyon with $h/H = 0.25$ (Fig.6 g) with respect to $h/H = 0.50$ case (Fig. 6h) are been observed.

Actually, the flow is far from being stationary and the shear layer is dominated by intermittent events, namely sweeps and ejections, which allow periodic flux exchanges between canyon and

overlaying air. The intermittent behaviour, which has a key role in canyon ventilation, has been investigated for flat roof buildings (e.g. Cheng and Liu 2011; Kikumoto and Ooka 2012), whilst gable roof configurations have not been properly analysed yet. Although a characterization of the non-stationary behaviour goes beyond the scope of this work, it is worthwhile pointing out that it should be amplified by roof presence.

Intermittency is apparent when analysing the concentration snapshots (here not reported): the plume changes direction, thus the pollution entering the canyon varies in direction and magnitude. This behaviour has an effect also on the variance fields. Figure 7 shows, as an example, concentration variance field for gable roofs and chimneys in the leeward position: $h/H = 0.25$ (a) and 0.5 (b), (corresponding to the mean concentration fields in Fig. 6 g, h).
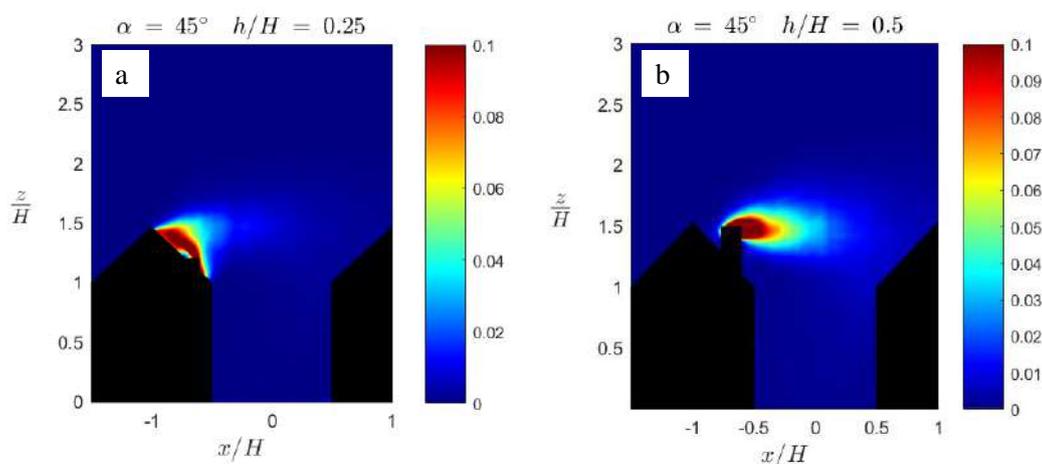

Figure 7: concentration variance made non dimensional with the maximum concentration registered at the source point, for 45° gable roof cases with chimney in the leeward position. (a) chimney height h/H = 0.25; (b) chimney height h/H = 0.5.

Differences between the two variance maps are apparent and they partially explain the lower mean canyon concentration of the case portrayed in Fig. 7a with respect to the one displayed in Fig. 7b. Indeed, Fig. 7a presents two high variance regions: one positioned above the chimney and the other behind the chimney. The pattern is the result of the oscillation of the plume axis whose position roughly oscillates around the chimney. When the plume reachs the top of the roof, it jumps to higher levels where turbulence is higher, while when it deflects the pollutant goes into the canyon vortex and remains there for a longer time. When the chimney height increases (Fig. 7b), the variance pattern is similar, and the maximum variations are visible around the source point, but the same shape of the concentration field is preserved. This is the typical behaviour, also found for the other analysed cases, both in case of flat and gable roof.

4. Conclusions

We experimentally investigated concentration fields with pollutants emitted by chimneys in a street canyon configuration with $AR_C = AR_B = 1$. A total of 9 cases were set-up by varying the roof shape (flat and gable roof, 45° pitch), the chimney height ($h/H = 0.25, 0.50, 0.75$) and the chimney position on the roof (mid point in case of flat roof, leeward and windward position in case of gabled roof). Analyses were carried on in a water flume and the non-intrusive image techniques FTV (Feature Tracking Velocimetry) and LIF (Light Induced Fluorescein) were applied. Results demonstrated that no trivial mixing mechanism occurs because of the coupled effect of the roof shape and chimney configuration. Quite obviously, increasing the chimney height leads to benefits with respect the canyon pollution. Among the simulated configurations, the minimum mean concentration value inside

the canyon is achieved for the highest chimney and flat roofs, since the interaction with the underlying canopy is minimized in that case. Considering gable roof cases, the windward position is preferable with respect to the leeward one. When the chimney is in leeward position, oppositely to what one might expect, mean concentration decreases considering the shortest chimney instead of the medium one. However, this work represents a first step in analysing this kind of problem and deeper studies should be done to better understand the phenomenon. For instance, intermittent flow behaviour, and its effect on the concentration field should be investigated. Besides, 3D effects and plume meandering are not captured by planar measurements and more complex features and non-trivial effects would arise if considering plume buoyant effects. Despite inherent simplifications, results suggest that caution has to be exercised when pollutant emissions are released from above the roofs, since the identification of the optimal solution, aimed at maximising dispersion at higher levels, while preserving the canyon air quality, is far from being obvious.

References

Badas MG, Ferrari S, Garau M, Querzoli G (2017) On the effect of gable roof on natural ventilation in two-dimensional urban canyons. Journal of Wind Engineering and Industrial Aerodynamics 162:24–34. doi: 10.1016/j.jweia.2017.01.006

Badas MG, Querzoli G (2011) Spatial structures and scaling in the Convective Boundary Layer. Exp Fluids 50:1093–1107. doi: 10.1007/s00348-010-1020-z

Bagieński Z (2006) The analysis of dispersion of pollutants from short point sources - wind tunnel experimental investigation. Environment Protection Engineering 37–45

Barlow JB, Rae WH, Pope A (1999) Low-Speed Wind Tunnel Testing. Wiley

Besalduch LA, Badas MG, Ferrari S, Querzoli G (2013) Experimental Studies for the characterization of the mixing processes in negative buoyant jets. EPJ Web of Conferences 45:01012. doi: 10.1051/epjconf/20134501012

Besalduch LA, Badas MG, Ferrari S, Querzoli G (2014) On the near field behavior of inclined negatively buoyant jets. EPJ Web of Conferences 67:02007. doi: 10.1051/epjconf/20146702007

Britter RE, Hanna SR (2003) Flow and Dispersion in Urban Areas. Annual Review of Fluid Mechanics 35:469–496. doi: 10.1146/annurev.fluid.35.101101.161147

Brown MJ, Lawson RE, Decroix DS, Lee RL (2000) Mean Flow and Turbulence Measurements Around a 2-D Array of Buildings in a Wind Tunnel. http://permalink.lanl.gov/object/tr?what=info:lanl-repo/lareport/LA-UR-99-5395. Accessed 19 Jun 2017

Carpentieri M, Hayden P, Robins AG (2012) Wind tunnel measurements of pollutant turbulent fluxes in urban intersections. Atmospheric Environment 46:669–674. doi: 10.1016/j.atmosenv.2011.09.083

Cheng WC, Liu C-H (2011) Large-Eddy Simulation of Flow and Pollutant Transports in and Above Two-Dimensional Idealized Street Canyons. Boundary-Layer Meteorol 139:411–437. doi: 10.1007/s10546-010-9584-y

Di Bernardino AD, Monti P, Leuzzi G, et al (2017) Experimental investigation of turbulence and dispersion around an isolated cubic building. pp 460–464

Di Bernardino AD, Monti P, Leuzzi G, Querzoli G (2015) Water-Channel Study of Flow and Turbulence Past a Two-Dimensional Array of Obstacles. Boundary-Layer Meteorol 155:73–85. doi: 10.1007/s10546-014-9987-2

Ferrari S, Badas MG, Garau M, et al (2016) The air quality in two-dimensional urban canyons with gable roof buildings: A numerical and laboratory investigation. pp 351–356

Ferrari S, Badas MG, Garau M, et al (2017) The air quality in narrow two-dimensional urban canyons with pitched and flat roof buildings. International Journal of Environment and Pollution 62:347–368. doi: 10.1504/IJEP.2017.089419

Garau M, Badas MG, Ferrari S, et al (2018a) Turbulence and Air Exchange in a Two-Dimensional Urban Street Canyon Between Gable Roof Buildings. Boundary-Layer Meteorology 167:123–143. doi: 10.1007/s10546-017-0324-4

Garau M, Badas MG, Ferrari S, et al (2018b) Air Exchange in urban canyons with variable building width: a numerical LES approach. Special Issue: HARMO18 (Under review)

Garau M, Grazia B, Ferrari S, et al (2017) The air quality in urban canyons with tight and wide buildings. pp 470–474

Ghermandi G, Fabbi S, Zaccanti M, et al (2015) Micro–scale simulation of atmospheric emissions from power–plant stacks in the Po Valley. Atmospheric Pollution Research 6:382–388. doi: 10.5094/APR.2015.042

Hajra B, Stathopoulos T, Bahloul A (2010) Assessment of pollutant dispersion from rooftop stacks: ASHRAE, ADMS and wind tunnel simulation. Building and Environment 45:2768–2777. doi: 10.1016/j.buildenv.2010.06.006

Ho Y-K, Liu C-H, Wong MS (2015) Preliminary study of the parameterisation of street-level ventilation in idealised two-dimensional simulations. Building and Environment 89:345–355. doi: 10.1016/j.buildenv.2015.02.042

Kikumoto H, Ooka R (2012) A numerical study of air pollutant dispersion with bimolecular chemical reactions in an urban street canyon using large-eddy simulation. Atmospheric Environment 54:456–464. doi: 10.1016/j.atmosenv.2012.02.039

Llaguno-Munitxa M, Bou-Zeid E, Hultmark M (2017) The influence of building geometry on street canyon air flow: Validation of large eddy simulations against wind tunnel experiments. Journal of Wind Engineering and Industrial Aerodynamics 165:115–130. doi: 10.1016/j.jweia.2017.03.007

Mahjoub Saïd N, Mhiri H, Le Palec G, Bournot P (2005) Experimental and numerical analysis of pollutant dispersion from a chimney. Atmospheric Environment 39:1727–1738. doi: 10.1016/j.atmosenv.2004.11.040

Nosek Š, Kukačka L, Kellnerová R, et al (2016) Ventilation Processes in a Three-Dimensional Street Canyon. Boundary-Layer Meteorol 159:259–284. doi: 10.1007/s10546-016-0132-2

Nosek Š, Libor K, Klara J, et al (2017) Impact of roof height non-uniformity on pollutant transport between a street canyon and intersections

Oke TR (1988) Street design and urban canopy layer climate. Energy and Buildings 11:103–113. doi: 10.1016/0378-7788(88)90026-6

Ricci A, Kalkman I, Blocken B, et al (2017) Local-scale forcing effects on wind flows in an urban environment: Impact of geometrical simplifications. Journal of Wind Engineering and Industrial Aerodynamics 170:238–255. doi: 10.1016/j.jweia.2017.08.001

Saathoff P, Gupta A, Stathopoulos T, Lazure L (2009) Contamination of fresh air intakes due to downwash from a rooftop structure. J Air Waste Manag Assoc 59:343–353

Schulman LL, Strimaitis DG, Scire JS (2000) Development and Evaluation of the PRIME Plume Rise and Building Downwash Model. Journal of the Air & Waste Management Association 50:378–390. doi: 10.1080/10473289.2000.10464017

Snyder WH (1972) Similarity criteria for the application of fluid models to the study of air pollution meteorology. Boundary-Layer Meteorol 3:113–134. doi: 10.1007/BF00769111

Willis GE, Deardorff JW (1983) On plume rise within a convective boundary layer. Atmospheric Environment (1967) 17:2435–2447. doi: 10.1016/0004-6981(83)90068-9